



Published in final edited form as:

Annu Rev Pathol. 2018 January 24; 13: 379–394. doi:10.1146/annurev-pathol-051217-111018.

The glymphatic system in CNS health and disease: past, present and future

Benjamin A. Plog^{1,2,#} and Maiken Nedergaard¹

¹Center for Translational Neuromedicine, Department of Neurosurgery, University of Rochester Medical Center, Rochester, NY 14642, USA

²Department of Pathology, University of Rochester Medical Center, Rochester, NY 14642, USA

Abstract

The central nervous system (CNS) is unique in being the only organ system lacking lymphatic vessels to assist in the removal of interstitial metabolic waste products. Recent work has led to the discovery of the glymphatic system, a glial-dependent perivascular network that subserves a pseudo-lymphatic function in the brain. Within the glymphatic pathway, cerebrospinal fluid (CSF) enters brain via periaxonal spaces, passes into the interstitium via perivascular astrocytic aquaporin-4, and then drives the perivenous drainage of interstitial fluid (ISF) and its solute. Here we review the role of the glymphatic pathway in CNS physiology, factors known to regulate glymphatic flow, and pathologic processes where a breakdown of glymphatic CSF-ISF exchange has been implicated in disease initiation and progression. Important areas of future research, including manipulation of glymphatic activity aiming to improve waste clearance and therapeutic agent delivery, will also be discussed.

Keywords

Glymphatic; cerebrospinal fluid; perivascular space; aquaporin-4; amyloid- β ; astrocyte

INTRODUCTION

Within the central nervous system (CNS), approximately 60–68% of total water content falls within the intracellular space, while the remaining 32–40% occupies the extracellular compartment (1). The extracellular fluid can then be further divided into interstitial fluid (ISF), which surrounds the cells of the parenchyma and represents 12–20% of brain water, and the cerebrospinal fluid (CSF) and blood compartments, each comprising 10% of the intracranial water volume (1). In peripheral organs, products of cellular metabolism released into the ISF, as well as colloids and fluid filtered across a fenestrated capillary bed, are cleared to the venous blood through a network of lymphatic vessels that run in parallel to the

[#]Corresponding Author: Benjamin A. Plog, MS, Center for Translational Neuromedicine, Department of Neurosurgery, University of Rochester Medical Center, 601 Elmwood Ave, Box 80, Rochester, NY 14642, benjamin_plog@urmc.rochester.edu.

Disclosure Statement

The authors are not aware of any affiliations, memberships, funding, or financial holdings that might be perceived as affecting the objectivity of this review.

blood supply (2, 3). The CNS, however, is the only organ of the body that lacks anatomically defined lymphoid tissues (2), and as a result, has developed unique adaptations for achieving fluid balance and interstitial waste removal. In addition to its traditionally identified role providing buoyancy to the brain and thus protecting it from the rigid surrounding skull, the CSF has also been suggested to function as a pseudo-lymphatic system, acting as a sink for brain interstitial solute, particularly high molecular weight substances such as proteins (4, 5). Consequently, this review will focus on the efforts that have been made to identify the anatomical pathways and physiologic regulation governing the interaction between the CSF and ISF, the role of CSF-ISF exchange in neurophysiology and the promotion of extracellular homeostasis, and how the breakdown of this exchange may result from and contribute to diseases of the CNS, as well as have implications for the diagnosis and treatment of these diseases.

CSF – FORMATION AND CIRCULATION

CSF is formed by the choroid plexuses, protrusions of the ependymal lining of the lateral, third and fourth cerebral ventricles (6). The choroid plexuses are highly vascularized tissues characterized by a stroma embedded with fenestrated capillaries and surrounded by a single layer of secretory epithelial cells (7, 8). The absence of tight junctions between endothelial cells makes the choroid plexuses one of the few places within the CNS devoid of a blood-brain barrier (BBB), and this permits the movement of crystalloids, colloids, and fluid from the blood into the stroma down hydrostatic and osmotic pressure gradients (8). The secretion of CSF, however, is selective and regulated due to the presence of tight junctions between epithelial cells, thereby preventing the paracellular movement of most solutes into the ventricular lumen, and dividing the epithelial cell into an apical and basolateral membrane (8–10). To increase the surface area for solute and water transport, the basolateral membrane is highly folded and the epithelial apical membrane consists of a dense brush border of microvilli (7). For a comprehensive treatment of choroidal CSF secretion see (8); for purposes of this discussion, the major molecular species involved in this process will be briefly reviewed.

The principal ions transported by the choroid plexus are Na^+ , HCO_3^- , Cl^- and K^+ (1, 11). Primary active transport by the apical membrane Na^+/K^+ -ATPase (12, 13), pumping Na^+ out of and K^+ into the cell up their concentration gradients, generates the requisite energy for all other secondary active transport processes, and inhibition of this enzyme with ouabain has been shown to reduce CSF production 70–80% in dog and rabbit (14, 15). Due to its low intracellular and high blood concentration, Na^+ will enter the epithelial cell via the basolateral Na^+ -dependent $\text{Cl}^-/\text{HCO}_3^-$ exchanger (NCBE), the $\text{Na}^+/\text{HCO}_3^-$ co-transporter (NBCn1/2) or the Na^+/H^+ exchanger (NHE1) (1, 8, 11–13). These transporters, as well as cytoplasmic carbonic anhydrase, will increase intracellular HCO_3^- , which can then move into the ventricular CSF by the apical $\text{Na}^+/\text{HCO}_3^-$ co-transporter (NBCe2), or can drive basolateral Cl^- entry through the $\text{Cl}^-/\text{HCO}_3^-$ anion exchanger (AE2) (1, 8, 11–13). Passage of Cl^- into the ventricular lumen has been described to occur via the apical K^+/Cl^- co-transporter (KCC4), or the electroneutral apical $\text{Na}^+/\text{K}^+/2\text{Cl}^-$ co-transporter (NKCC1) (1, 8, 11–13). The net transit of Na^+ , HCO_3^- and Cl^- from the blood to the ventricular lumen establishes an osmotic gradient that will also drive water across the epithelial membrane.

The movement of water is facilitated by a high apical, and lower basolateral, expression of aquaporin-1 (AQP1) (12, 13, 16–18). Interestingly, genetic deletion of AQP1 only reduces CSF production by 25% (19, 20), suggesting alternative mechanisms for water transport, including paracellular and transcellular diffusion, and as a requisite co-transport molecule. As an example, it has been demonstrated that for every turnover of NKCC1, 590 water molecules are transported alongside the four ionic osmolytes (21). Additionally, the glucose transporter, GLUT1, is highly expressed in the basolateral membrane of choroidal epithelial cells (22), potentially to support the high metabolic rate of this secretory tissue, but it has also been suggested their presence is to facilitate water co-transport, thereby increasing the water permeability of the cell required for CSF secretion (11, 23, 24).

Collectively, this molecular machinery produces 500–600 mL of CSF each day in humans (4, 8). Following production, CSF will flow from the lateral ventricles to the third via the foramina of Monro, continue to the fourth by passing through the cerebral aqueduct, and ultimately enters the subarachnoid space and cisterns via the midline foramen of Magendie and the two lateral foramina of Luschka (8). In order to fulfill its posited lymphatic function, subarachnoidal CSF must then be able to enter brain to renew ISF, and ISF and solute must be able to drain back to the CSF to achieve waste removal and volume homeostasis. Consequently, the pathways facilitating these fluid dynamics have been an intense area of study over the past several decades.

PERIVASCULAR SPACES – CONDUITS FOR FLUID MOVEMENT INTO AND OUT OF BRAIN

In early work attempting to elaborate the anatomy of ISF drainage from the CNS, traceable solutes were injected directly into the brain parenchyma and then, after allowing various periods of time to elapse, the distribution of these molecules was evaluated, assuming they would label pathways of ISF exit from the tissue. In the first of these studies, Blue Dextran 2000 was injected to the caudate nucleus of rats, and at both 15 minutes and 24 hours it was observed that this dye did not disperse isotropically from the injection site, but rather seemed to preferentially move in certain directions along what appeared to be cerebral blood vessels (25). To more clearly localize the sites of interstitial solute efflux, horse radish peroxidase (HRP) was again injected to the rat striatum, and after allowing 4–8 hours for spread within the extracellular spaces of the brain, it was noted that there was significant appearance of this tracer molecule within perivascular spaces (26). It was demonstrated that this perivascular drainage of interstitial fluid and solute was, at least in part, directed to the subarachnoid CSF (26, 27), and further, that perivascular ISF removal was ubiquitous throughout the brain, occurring in disparate regions beyond the caudate nucleus, including cerebral cortex, midbrain, and inferior colliculus (25–28).

There are several potential mechanisms by which fluids and the solutes contained therein may move within the brain. The first of these is diffusion, a passive process of stochastic Brownian motion that derives its energy not from metabolism, but from the thermal energy of the surrounding environment. At a constant physiologic temperature, diffusion can be thought of as a series of random molecular walks dependent upon the molecular size, the

concentration gradient, and the distance over which diffusion is occurring (29). Conversely, advection, also referred to as bulk flow, is an active process requiring energy from cellular metabolism to produce hydrostatic, electrical, or chemical gradients that can then drive the bulk movement of a fluid. Whereas small molecules tend to diffuse faster than larger molecules, advection has no molecular size dependence and all molecules are predicted to move at a rate equal to the flow of the fluid body (29). When both diffusive and advective processes govern molecular dynamics, this is referred to as convection (29). There has been much debate regarding whether the efflux of interstitial fluid, and its constituent solute, from brain are diffusion limited or driven by advection. When different molecular weight tracers, including albumin (69 kDa) and polyethylene glycols (4 kDa and 900 Da), were injected to the caudate nucleus of rats, despite there being an approximately five-fold difference in diffusion coefficients between these molecules, all were cleared with a nearly equivalent half-time of disappearance (26, 30). From this it was concluded that perivascular ISF drainage occurred by bulk fluid flow, as opposed to diffusion, and the rate of this flow was determined to be 0.1–0.3 $\mu\text{L/g}$ brain/min (27, 30, 31).

With compelling evidence that perivascular spaces serve as low resistance channels for ISF egress from brain to CSF, Rennels and colleagues next sought to determine if CSF could move from the subarachnoid compartment into the cerebral interstitial spaces, and if so, to identify the pathway of this influx. Here it was determined that within 4–10 minutes of delivery to the subarachnoid CSF, there was significant appearance of HRP within the perivascular spaces of cerebral blood vessels all the way down to the level of the microvascular basement membranes (32, 33). As a result, the authors concluded that CSF can penetrate the brain parenchyma using the same perivascular conduits ISF employs for drainage back to the CSF, and that this was likely a bulk flow-mediated process due to the rapidity of influx (32, 33). Interestingly, this same group found that influx of CSF within these perivascular spaces was significantly impaired within edematous cerebral tissues (34), suggesting that under normal conditions there is a pressure differential between the CSF and the tissue which facilitates movement into the brain, and that this can be ablated by increasing tissue water content and pressure. In a later study from Ichimura and colleagues where tracer molecules were micro-injected into the perivascular spaces of surface vessels, it was observed that the direction of flow was variable, with a vector into the brain along one segment of an artery and out of the brain in a more distal segment (35), thus challenging this concept of CSF penentrance into brain within perivascular channels.

THE GLYMPHATIC SYSTEM – A PATHWAY FOR CSF-ISF EXCHANGE

Anatomical organization

In a more recent study, fluorescently labeled dextrans were injected into the cisternal CSF of mice and it was observed that within 30 minutes there was robust perivascular labeling (36), confirming Rennels' prior work (32, 33). Using intravital 2-photon microscopy, these fluorescent CSF tracers rapidly appeared, as early as 5 minutes following injection, within the perivascular spaces of surface arteries, and then, over the subsequent 25 minutes, moved progressively deeper into the parenchyma within the perivascular spaces of penetrating arteries (36). In Tie2-GFP:NG2-DsRed double reporter mice, with labeled endothelial and

smooth muscle cells, respectively, it was found that fluorescent ovalbumin entered the brain specifically within the periarterial space between the smooth muscle and the astrocyte end-feet of the glial limiting membrane. At 3 hours following cisterna magna injection of the fluorescent ovalbumin, tracer could be identified within the basement membranes of parenchymal capillaries and in the perivascular spaces of large caliber draining veins, including the internal cerebral and caudal rhinal veins (36). Thus, not only was perivascular influx of CSF validated, but a directionality to this fluid movement was demonstrated, with CSF entering the brain exclusively within periarterial spaces and ISF leaving the brain within perivenous channels (36).

The role of aquaporin-4 water channels

Within the CNS, aquaporin-4 (AQP4) is a water channel predominantly expressed within astrocytic processes forming the subpial and subependymal glial limiting membranes, as well as the perivascular astrocytic end-foot processes circumscribing the entirety of the cerebrovasculature (16, 37). Tetramers of AQP4 assemble into supramolecular structures referred to as square arrays or orthogonal arrays of particles (OAPs) (16, 37). The shorter M23 isoform of AQP4, through intermolecular N-terminal interactions, forms the core of these OAPs, while the M1 isoform is restricted to the perimeter of the arrays (16). OAPs segregate to the plasma membrane of perivascular end-foot processes due to their association with the dystrophin-associated protein complex (DAPC). AQP4 is anchored to the DAPC through α -syntrophin, and the DAPC is in turn attached to laminin and agrin in the perivascular glial basement membrane via α -dystroglycan (37). As a consequence of this complex molecular organization, there is an unusually high density of these water channels positioned at the interface between the perivascular and interstitial spaces of the brain.

It has been posited that this localization of AQP4 channels functions to decrease the resistance to CSF-ISF exchange. Testing this assumption, Iliff and colleagues injected a fluorescent ovalbumin to the cisterna magna of global AQP4 knockout mice and found significantly reduced CSF influx relative to wildtype animals (36). Interestingly, compartmental analysis revealed that influx within periarterial spaces was unperturbed in the mice lacking AQP4, however, there was significantly impaired flow of the tracer from these spaces to the surrounding parenchyma (36), supporting the idea that these channels facilitate fluid movement between the perivascular and interstitial spaces. Further, intrastriatal injection of radiolabeled mannitol revealed that the rate of fluid and solute clearance from the brain's interstitial spaces was significantly suppressed in the knockout mice (36). Consequently, due to its dependence on the glial AQP4 channel, and pseudo-lymphatic function, Nedergaard's group named this pathway of periarterial CSF inflow and perivenous ISF and solute drainage, the glial-associated lymphatic pathway, or glymphatic pathway (36) (Fig. 1).

Post-glymphatic clearance pathways

Historically, subarachnoid CSF, and the ISF that drains into this compartment, have been thought to leave the cranium via the one-way valve arachnoid granulations, which release CSF into the dural venous sinuses (38). It has also been demonstrated, however, that a significant proportion of CSF can exit the cranial vault along the internal carotid artery (39),

as well as within the perineural spaces of cranial nerves, including the vagal and olfactory nerves (39, 40). In particular, extensions of the subarachnoid space that follow the olfactory tracts, cross the cribriform plate, and project into the nasal submucosa alongside olfactory nerves, have been shown to be responsible for 15–30% of the removal of CSF solute (41). There is a dense lymphatic network within the nasal submucosa that then drains this CSF and solute to the deep cervical lymph nodes (dcLNs) (41). This pathway of clearance to the dcLNs is especially important for large molecular weight molecules, as solutes under 5 kDa are capable of passing from CSF to blood directly across the microvascular wall within the nasal submucosa (42). Up to 50% of radioiodinated serum albumin (RISA) injected to the caudate nucleus drains via the olfactory-nasal submucosa-dcLN pathway, suggesting that this may be the dominant egress site for interstitial solutes (43), however, there is also anatomical variability in the magnitude of ISF clearance to the dcLNs that may be reflective of distance from the olfactory bulbs. Illustrating this point, only 22% and 18% of RISA injected to the internal capsule and the more caudal midbrain, respectively, could be collected in the deep cervical lymph (44). Efflux of CSF and ISF to the dcLNs is likely critical for intracranial volume regulation, waste removal, and neuroimmunology, as it has been shown to be evolutionarily conserved across mammalian species ranging from mice to non-human primates to humans (45, 46).

More recent evidence has challenged the paradigm of the CNS being devoid of lymphatic vessels. In studies by Louveau *et al* and Aspelund *et al*, vessels with structural, molecular, and functional similarities to peripheral lymphatic vessels were identified immediately adjacent to dural sinuses, including the superior sagittal sinus and the transverse sinuses, as well as aligning the meningeal vascular supply, such as the middle meningeal artery (47, 48) (Fig. 2). It was shown that fluorescent tracers, delivered either intracerebroventricular or intraparenchymal, could be identified within the lumen of these dural lymphatics, and that ultimately these vessels drained to the dcLNs (47, 48). Ligation of the afferent lymphatic vessel to the dcLNs led to dilation of the meningeal vessels, suggesting upstream congestion (47), and genetic ablation of the meningeal lymphatics significantly impaired clearance of CSF-based tracer to the dcLNs (48). Questions persist, however, regarding whether these vessels are positioned within the dural membrane, or rather lie at the interface between the dura and the subarachnoid space, and further, the mechanism by which CSF and solute can traverse the dura and the wall of these vessels to arrive within the lumen remains to be elaborated (49).

Regulation of glymphatic flow

Physiologic regulation of glymphatic pathway function is multifaceted. Iliff and colleagues were able to demonstrate that ligation of the internal carotid artery, dampening cardiac cycle-related pulsatility of cortical penetrating arteries, led to impaired glymphatic CSF tracer influx into cerebral tissues (50). Conversely, when dobutamine, an inotropic adrenergic agonist, was systemically given to mice it was found that the penetrating arterial pulsatility index was increased, and that this was associated with significantly more CSF tracer penetrance into brain (50). Consequently, the authors concluded their metric of penetrating arterial pulsatility, which integrated changes related to amplitude and frequency of diameter oscillation, was positively associated with CSF influx within the glymphatic

pathway (50). Interestingly, in a separate study it was found that partial occlusion of the brachiocephalic artery, to eliminate pulsatility while maintaining blood flow in the carotid artery, also led to impaired movement of subarachnoid CSF into brain (32). These findings were supported by later work using ultra-fast magnetic resonance encephalography that demonstrated cardiac cycle-related pulsatility was responsible for driving periarterial CSF from the circle of Willis centrifugally toward the dorsal cortical surface (51). This same study also identified a role for respiratory cycle-related pulsatility in centripetal perivenous fluid movements, as well as fluid dynamics related to very low frequency vasomotor oscillations (51).

It has also been demonstrated that level of arousal plays an important role in governing glymphatic CSF and ISF dynamics. Natural sleep was associated with enhanced periarterial CSF tracer influx and improved interstitial solute clearance, including soluble amyloid- β (A β) (52). These findings were recapitulated in anesthetized mice, suggesting that changes in glymphatic transport were related to state of consciousness and not circadian rhythms (52). Increased glymphatic function in the sleep state was determined to result from an increased interstitial space volume fraction, and this in turn was found to be a consequence of lower locus coeruleus-derived noradrenergic tone (52). As a result, here it was concluded that in the transition from wakefulness to sleep, as central norepinephrine levels decline, the extracellular space expands, and the resultant decrease in tissue resistance leads to faster CSF influx and interstitial solute efflux (52). In a separate study, it was found that head position during sleep also modifies flow through this pathway. Here, using dynamic-contrast-enhanced MRI, it was found that there was lower interstitial solute retention and improved clearance when mice were placed in the lateral decubitus position compared to either prone or supine positions (39). Further, it was demonstrated that there was enhanced fluorescent CSF tracer influx to the cerebrum when mice were placed in the lateral position relative to being prone (39). Thus, it is clear that postural or gravitational factors also exert regulatory control over the glymphatic pathway.

Functions of the glymphatic system

Glymphatic CSF-ISF exchange has been demonstrated to perform a number of roles in neurophysiology. Perhaps most central to this pathway's lymphatic function is its waste clearance capacity. In AQP4 knockout mice with reduced glymphatic function, the clearance of interstitial solutes, including mannitol and A β , has been observed to be significantly impaired (36). Additionally, it was found that enhanced glymphatic clearance is responsible for the reduced brain lactate levels that accompany the transition from wakefulness to sleep. Here, inhibition of glymphatic clearance in anesthetized mice, either with AQP4 deletion, acetazolamide therapy, cisterna magna puncture, or changes in head position, led to higher brain and lower cervical lymph node lactate levels (53). Beyond clearance, this pathway has been shown to be critical for the distribution of nutrients, such as glucose, throughout the brain (54), and for the delivery of therapeutic agents, as reduced viral transduction was demonstrated following intracerebroventricular injection of AAV9-GFP in AQP4 knockout mice (55). Further, bulk flow through the glymphatic pathway contributes to volume transmission and paracrine signaling. It was found that suppression of glymphatic flow with cisterna magna puncture impaired perivascular lipid transport, and as a consequence

spontaneous astrocytic Ca^{2+} signaling within the awake cortex became more frequent, but with reduced synchronization (56). Finally, in a recent study, it was found that fluid shear stress, analogous to that produced by perivascular CSF or ISF dynamics, is capable of mechanically opening NMDA receptors on cultured astrocytes, producing increased Ca^{2+} current (57), and suggesting a role for glymphatic flow in mechanotransduction.

Glymphatic dysfunction in CNS disease

With multiple critical roles in CNS physiology, it is perhaps not surprising that dysfunction of the glymphatic pathway has been implicated in a variety of neurologic diseases, particularly those where accumulation of pathologic solute is a prominent feature. It has been demonstrated that there is an age-associated decline in glymphatic CSF influx, as well as interstitial solute clearance, including $\text{A}\beta$, and this appears to be related to reduced penetrating arterial pulsatility in the aged brain (58). In the context of Alzheimer's disease (AD), young APP/PS1 double transgenic mice, expressing chimeric mouse/human amyloid precursor protein (Mo/HuAPP695swe) and a mutant form of human presenilin-1 (PS1-dE9), were found to have both reduced glymphatic influx and clearance of $\text{A}\beta$, and this was shown to worsen as a function of age (59). Further, pretreatment of wildtype mice with $\text{A}\beta$ led to significant suppression of CSF tracer influx, suggesting that not only does AD lead to reduced glymphatic clearance and accumulation of $\text{A}\beta$, but that this $\text{A}\beta$ aggregation will feed forward and produce further glymphatic slowing (59). Decreased glymphatic influx has also been observed secondary to subarachnoid hemorrhage, acute ischemia, and multiple micro-infarction (60, 61). Interestingly, in the case of multiple small embolic strokes, while glymphatic perfusion spontaneously recovers by 14 days, there is persistent solute trapping within lesion cores, potentially explaining the clinical connection between this disease, $\text{A}\beta$ plaque formation, and long-term neurodegeneration (61). In the murine 'Hit & Run' model of traumatic brain injury (TBI), impairment of glymphatic CSF inflow to brain is seen between 1 and 28 days following injury (Fig. 3), and solute clearance from the cortical interstitium is slowed at 7 days (62). When there is a second hit to the glymphatic system, and TBI is provided in AQP4 knockout mice, solute clearance is even further suppressed, showing a significant reduction relative to wildtype TBI mice (62). Functionally, post-traumatic glymphatic failure, particularly in *Aqp4*^{-/-} mice, is associated with significant motor, object memory, and spatial memory deficits (62). All of the previously discussed diseases are characterized by astrogliosis, measured by increased glial fibrillary acidic protein (GFAP) expression, and this has been shown to drive a loss of perivascular AQP4 localization, potentially representing a common mechanism of glymphatic dysfunction in these pathologies (58, 59, 61, 62) (Fig. 4). Thus far, type II diabetes mellitus is the only disease process characterized by enhanced glymphatic CSF influx and slowed interstitial solute clearance, and the magnitude of this mismatched inflow and outflow has been correlated with degree of cognitive decline (63). Due to its pathophysiologic contribution to such a broad segment of CNS diseases, the glymphatic system represents an important target for therapeutic intervention. As known regulatory elements have yet to yield glymphatic-directed treatment strategies, further work is necessary to uncover novel regulation of this pathway.

FUTURE DIRECTIONS OF STUDY

Cerebral ISF formation as a novel target for therapeutic regulation of glymphatic function

Whereas in peripheral organs ISF is formed as a product of hydrostatic filtration of blood plasma through a fenestrated capillary bed, owing to the presence of tight junctions between adjacent endothelial cells of the BBB (9, 64), the same is not true in the CNS, where ISF is instead actively secreted by the cerebrovascular endothelium (11). The endothelial layer of brain blood vessels is thought to behave analogously to the epithelium of the choroid plexus, and has been noted to have an increased mitochondrial content relative to peripheral endothelial cells to energetically support this secretory function (65). Here, the secretion of ISF will be discussed with respect to only those proteins that have been molecularly and functionally identified and localized to either the luminal or abluminal membrane of the endothelial cell; for a more comprehensive review, see (11). Similar to the choroid epithelium, the Na^+/K^+ -ATPase is positioned on the secretory, abluminal surface of the endothelial cell, driving Na^+ into the brain's interstitial space and pumping K^+ back into the cell (11). The establishment of a low intracellular concentration of Na^+ relative to the blood plasma allows Na^+ to then enter the cell down this gradient via the luminal Na^+/H^+ exchangers (NHE1/2) or the $\text{Na}^+/\text{K}^+/\text{2Cl}^-$ co-transporter (NKCC1) (11). At present, it is not clear how Cl^- traverses the abluminal membrane to maintain electroneutrality with Na^+ , however, a role for yet to be identified K^+/Cl^- co-transporters or Cl^- channels has been posited (11). While AQP1 facilitates water transport in capillary endothelial cells in peripheral organs, it is not expressed throughout the brain endothelium (16, 18), and further, it has been demonstrated that AQP4 channels are specific to the astrocyte end-foot, with no expression within the endothelial layer (16, 66). Consequently, water transport at the BBB is likely by co-transport alongside the ionic species previously discussed. While the rate of ISF secretion has proven difficult to determine, indirect measurement in choroid plexectomized animals has suggested that approximately 20% of the total CSF volume is secondary to ISF formation (8), and consequently, ISF secretion has historically been referred to as extrachoroidal CSF production.

Though ISF is formed in the perivascular and interstitial spaces that make up the glymphatic pathway, and drains in large part to the subarachnoid CSF compartment, surprisingly very little is known about how ISF production affects bulk fluid flow within this system. It has been posited in the literature that the CSF compartment can buffer changes in tissue volume that result from different rates of ISF secretion by the cerebrovascular endothelium (67). This model suggests that when ISF secretion declines and brain volume contracts, the bulk flow of CSF into brain is increased as a mechanism of replacing lost volume. In the alternative situation, however, when ISF secretion is increased, it has been proposed that the CSF compartment can act as a sink for excess fluid, and therefore, bulk movement of CSF into brain is reduced (67). Consequently, altering the rate of brain ISF secretion, potentially with pharmacology, may be an effective approach for both up and down-regulating glymphatic pathway function. Prior work from our group has demonstrated that changes in noradrenergic tone play a role in regulating glymphatic physiology (52). During wakefulness, elevated norepinephrine levels lead to a contraction in the extracellular space volume fraction, and the resultant increased interstitial resistance reduces both CSF influx,

as well as ISF and solute efflux from brain (52). Locus coeruleus-derived norepinephrine, however, has also been shown to increase BBB water permeability through increased activity of the endothelial abluminal Na^+/K^+ -ATPase (68, 69), thus effectively increasing ISF secretion, and potentially representing an alternative mechanism for slowed glymphatic kinetics during wakefulness. Consequently, centrally administered adrenergic agonists and antagonists may be an effective way of targeting norepinephrine-mediated ISF production, and thereby modulating glymphatic function. Additionally, the central hormone, arginine vasopressin (AVP), has been found to increase cerebral capillary water permeability and brain water content (70, 71), and antagonism of the cerebrovascular expressed V1a receptor has been shown to reduce cerebral edema following TBI (72). Interestingly, systemic administration of AVP did not reproduce these findings, suggesting that similar to other vasopressin-sensitive membranes, the BBB endothelium is only responsive on a single side, its abluminal secretory surface (70). As a result, targeting brain-derived AVP may represent another powerful tool in the control of cerebral ISF secretion and flow within the glymphatic pathway. Further, pharmacologic modulation of ISF secretion potentially allows for evaluation of the effect of high or low glymphatic flow, in the absence of superimposed pathology, on cellular and molecular neurobiology, including neuroinflammatory processes, as well as behavioral function.

These neuromodulatory and hormonal systems also may play a role in CNS pathology through their influence on BBB ISF secretion. For example, locus coeruleus degeneration is a prominent feature in Alzheimer's disease (73). While this would be predicted to lead to decreased norepinephrine levels within the brains of these patients, in fact, noradrenergic tone is elevated (74), suggesting that degeneration may disproportionately affect inhibitory interneurons. Consequently, this observation of increased central norepinephrine, and the predicted increase in ISF secretion, may explain the reduced glymphatic influx observed in the APP/PS1 Alzheimer's disease mice (59).

Modulation of ISF production to improve gene therapy and drug delivery within the CNS

While increased ISF production may be useful for improving the clearance of interstitial solutes from brain, low ISF formation, through enhancing glymphatic CSF influx, may represent a potential tool for increasing the transduction of intrathecally-delivered virally-packaged gene therapy, as well as the distribution of drugs, such as anti-neoplastic treatments, to a larger area of brain and to structures not in direct contact with the CSF compartment. In a recent study, it was demonstrated that the glymphatic system is responsible for the brain-wide delivery of an adeno-associated virus (AAV)-GFP construct, and that decreased glymphatic influx in AQP4 knockout mice resulted in reduced viral transduction and GFP expression (55). Additionally, it has been reported that AAV-mediated GFP labeling of primary sensory neurons was enhanced with intravenous mannitol pre-treatment prior to intrathecal virus injection (75). Consequently, an important area of future study will be in determining whether the mechanism of this improved transduction is through increased glymphatic CSF bulk flow, and if so, whether this can be used to functionally modify diseases with a known genetic etiology.

Elaboration of a three-dimensional glymphatic connectome within the intact CNS

The glymphatic pathway, because of the parallel nature with which it runs to the blood supply, spans the entirety of the CNS and is truly an organ-wide system (36, 40). Further, the annular perivascular channels and intervening interstitial spaces that constitute this pathway within the CNS are connected to the periphery via a number of post-glymphatic efflux sites, including arachnoid granulations (38), meningeal lymphatics (47, 48), perineural spaces of cranial and spinal nerves (39–41, 43), and potentially the soft tissues surrounding large vessels such as the internal carotid artery (39). Historically, fluid dynamics within the glymphatic pathway have been studied with either *in vivo* 2-photon laser scanning microscopy or *ex vivo* conventional fluorescence and confocal microscopy (36, 50, 52, 56, 58, 59, 62, 76). While 2-photon imaging is capable of providing dynamic information on perivascular flows and flows between the perivascular and interstitial spaces within the living subject (36), a narrow focal field and shallow focal depth precludes assessment of glymphatic function at a brain-wide level and in structures deeper than several hundred microns below the cortical surface. Conversely, *ex vivo* imaging modalities are better suited for evaluating CSF-ISF exchange simultaneously in disparate brain regions, in anatomical structures deep to the surface of the brain, and for evaluating cellular and molecular contributions to glymphatic function. This approach, however, does not provide any dynamic flow information. Additionally, removal of the brain from the skull dissociates the glymphatic system from post-glymphatic pathways, and sectioning of the cerebrum leads to disruption of glymphatic connections within the brain. Finally, while MRI coupled with intrathecal gadolinium-based contrast agents allows for dynamic, macroscopic imaging of glymphatic function throughout the whole brain, this modality is limited by poor anatomical resolution for micron-scale perivascular spaces and meningeal lymph vessels. Consequently, it is clear that novel technique development is required to study the glymphatic connectome, both at the level of the brain and spinal cord, as well as how this system communicates with peripheral organs throughout the body.

SUMMARY AND CONCLUSIONS

Glymphatic dysfunction characterized by a failure of interstitial solute clearance is a central feature of natural brain aging, as well as a broad segment of CNS diseases including Alzheimer's disease, TBI, and ischemic and hemorrhagic stroke (58–62). Additionally, in type II diabetes mellitus, an imbalance exists where there is increased glymphatic CSF influx without a concomitant increase in ISF efflux, thus leading to extracellular solute accumulation and cognitive decline (63). While much is known about the physiologic regulation of glymphatic pathway function, including the roles of cerebral arterial pulsatility (32, 50, 51), state of consciousness (52), and even head position (39), at present there are no glymphatic-directed therapies to intervene in any of these various disease processes. As a result, the primary goal of future studies will be the identification of a novel target for up or down-regulating CSF-ISF exchange within the glymphatic pathway, ultimately to promote improved solute clearance in diseases where metabolite accumulation is a prominent feature.

Acknowledgments

We would like to acknowledge Inglewood Biomedical Editing for assistance in the editing of this manuscript.

Literature Cited

1. Jessen NA, Munk ASF, Lundgaard I, Nedergaard M. The glymphatic system: A beginner's guide. *Neurochem Res.* 2015;1–17. [PubMed: 25366463]
2. Trevaskis NL, Kaminskas LM, Porter CJH. From sewer to saviour — targeting the lymphatic system to promote drug exposure and activity. *Nat Rev Drug Discov.* 2015; 14(11):781–803. [PubMed: 26471369]
3. Oliver G. Lymphatic vasculature development. *Nat Rev Immunol.* 2004; 4(1):35–45. [PubMed: 14704766]
4. Cserr HF. Physiology of the choroid plexus. *Physiol Rev.* 1971; 51(2):273–311. [PubMed: 4930496]
5. Hladky SB, Barrand MA. Mechanisms of fluid movement into, through and out of the brain: evaluation of the evidence. *Fluids Barriers CNS.* 2014; 11(26):1–32. [PubMed: 24467887]
6. Keep R, Jones H. A morphometric study on the development of the lateral ventricle choroid plexus, choroid plexus capillaries and ventricular ependyma in the rat. *Brain Res Developmental Brain Res.* 1990; 56(1):47–53.
7. Maxwell D, Please D. The electron microscopy of the choroid plexus. *J Biophys Biochem Cytol.* 1956; 2(4):467–74. [PubMed: 13357511]
8. Damkier HH, Brown PD, Praetorius J. Cerebrospinal fluid secretion by the choroid plexus. *Physiol Rev.* 2013; 93(4):1847–92. [PubMed: 24137023]
9. Brightman MW, Reese TS. Junctions between intimately apposed cell membranes in the vertebrate brain. *J Cell Biol.* 1969; 40(3):648–77. [PubMed: 5765759]
10. Kratzer I, Vasiljevic A, Rey C, Fevre-Montange M, Saunder N, et al. Complexity and developmental changes in the expression pattern of claudins at the blood-CSF barrier. *Histochem Cell Biol.* 2012; 138(6):861–79. [PubMed: 22886143]
11. Hladky SB, Barrand MA. Fluid and ion transfer across the blood-brain and blood-cerebrospinal fluid barriers; a comparative account of mechanisms and roles. *Fluids Barriers CNS.* 2016; 13(19):1–69. [PubMed: 26822521]
12. Praetorius J, Nielsen S. Distribution of sodium transporters and aquaporin-1 in the human choroid plexus. *Am J Physiol Cell Physiol.* 2006; 291(1):C59–67. [PubMed: 16481371]
13. Praetorius J. Water and solute secretion by the choroid plexus. *Pflugers Arch Eur J Physiol.* 2007; 454(1):1–18. [PubMed: 17120021]
14. Vates TJ, Bonting S, Oppelt W. Na-K activated adenosine triphosphatase formation of cerebrospinal fluid in cat. *Am J Physiol.* 1964; 206:1165–72. [PubMed: 14208960]
15. Pollay M, Hisey B, Reynolds E, Tomkins P, Stevens F, Smith R. Choroid plexus Na⁺/K⁺-activated adenosine triphosphatase and cerebrospinal fluid formation. *Neurosurgery.* 1985; 17(5):768–72. [PubMed: 2999636]
16. Papadopoulos MC, Verkman AS. Aquaporin water channels in the nervous system. *Nat Rev Neurosci.* 2013; 14:1–13. [PubMed: 23232605]
17. Johansson P, Dziegielewska K, Ek C, Habgood M, Møllgård K, et al. Aquaporin-1 in the choroid plexuses of developing mammalian brain. *Cell Tissue Res.* 2005; 322(3):353–64. [PubMed: 16133142]
18. Nielsen S, Smith B, Christensen E, Agre P. Distribution of the aquaporin CHIP in secretory and resorptive epithelia and capillary endothelia. *Proc Natl Acad Sci U S A.* 1993; 90(15):7275–79. [PubMed: 8346245]
19. Oshio K, Song Y, Verkman A, Manley G. Aquaporin-1 deletion reduces osmotic water permeability and cerebrospinal fluid production. *Acta Neurochirurgica Suppl.* 2003; 86:525–28.
20. Oshio K, Watanabe H, Song Y, Verkman A, Manley G. Reduced cerebrospinal fluid production and intracranial pressure in mice lacking choroid plexus water channel Aquaporin-1. *FASEB J.* 2005; 19(1):76–78. [PubMed: 15533949]
21. Stokum, Ja, Gerzanich, V., Simard, JM. Molecular pathophysiology of cerebral edema. *J Cereb Blood Flow Metab.* 2016; 36(3):513–38. [PubMed: 26661240]

22. Farrell C, Yang J, Pardridge W. GLUT-1 glucose transporter is present within apical and basolateral membranes of brain epithelial interfaces and in microvascular endothelia with and without tight junctions. *J Histochem Cytochem.* 1992; 40(2):193–99. [PubMed: 1552163]
23. Fischbarg J, Kuang K, Hirsch J, Lecuona S, Rogozinski L, et al. Evidence that the glucose transporter serves as a water channel in J774 macrophages. *Proc Natl Acad Sci U S A.* 1989; 86(21):8397–8401. [PubMed: 2813396]
24. Fischbarg J, Kuang K, Vera J, Arant S, Silverstein S, et al. Glucose transporters serve as water channels. *Proc Natl Acad Sci U S A.* 1990; 87(8):3244–47. [PubMed: 2326282]
25. Cserr HF, Ostrach LH. Bulk flow of interstitial fluid after intracranial injection of Blue Dextran 2000. *Exp Neurol.* 1974; 45(1):50–60. [PubMed: 4137563]
26. Cserr HF, Cooper DN, Milhorat TH. Flow of cerebral interstitial fluid as indicated by the removal of extracellular markers from rat caudate nucleus. *Exp Eye Res.* 1977:461–73. [PubMed: 590401]
27. Szentistvanyi I, Patlak CS, Ellis RA, Cserr HF. Drainage of interstitial fluid from different regions of rat brain. *Am J Physiol.* 1984; 246:F835–44. [PubMed: 6742132]
28. Ball KK, Cruz NF, Mrak RE, Dienel Ga. Trafficking of glucose, lactate, and amyloid-beta from the inferior colliculus through perivascular routes. *J Cereb Blood Flow Metab.* 2010; 30(1):162–76. [PubMed: 19794399]
29. Thrane AS, Rangroo Thrane V, Nedergaard M. Drowning stars: reassessing the role of astrocytes in brain edema. *Trends Neurosci.* 2014:1–9.
30. Cserr HF, Cooper DN, Suri PK, Patlak CS. Efflux of radiolabeled polyethylene glycols and albumin from rat brain. *Am J Physiol.* 1981; 240:F319–28. [PubMed: 7223889]
31. Abbott NJ. Evidence for bulk flow of brain interstitial fluid: significance for physiology and pathology. *Neurochem Int.* 2004; 45(4):545–52. [PubMed: 15186921]
32. Rennels ML, Gregory TF, Blaumanis OR, Fujimoto K, Grady PA. Evidence for a “paravascular” fluid circulation in the mammalian central nervous system, provided by the rapid distribution of tracer protein throughout the brain from the subarachnoid space. *Brain Res.* 1985; 326:47–63. [PubMed: 3971148]
33. Rennels ML, Blaumanis OR, Grady PA. Rapid solute transport throughout the brain via paravascular fluid pathways. *Adv Neurol.* 1990; 52:431–39. [PubMed: 2396537]
34. Blaumanis OR, Rennels ML, Grady PA. Focal cerebral edema impedes convective fluid/tracer movement through paravascular pathways in cat brain. *Adv Neurol.* 1990; 52:385–89. [PubMed: 2396535]
35. Ichimura T, Fraser PA, Cserr HF. Distribution of extracellular tracers in perivascular spaces of the rat brain. *Brain Res.* 1991; 545(1–2):103–13. [PubMed: 1713524]
36. Iliff JJ, Wang M, Liao Y, Plogg BA, Peng W, et al. A paravascular pathway facilitates CSF flow through the brain parenchyma and the clearance of interstitial solutes, including amyloid beta. *Sci Transl Med.* 2012; 4(147):1–11.
37. Nagelhus EA, Ottersen OP. Physiological roles of aquaporin-4 in brain. *Physiol Rev.* 2013; 93(4): 1543–62. [PubMed: 24137016]
38. Weed L. Studies on cerebro-spinal fluid. No III: The pathways of escape from the subarachnoid spaces with particular reference to the arachnoid Villi. *J Med Res.* 1914; 31(1):51–91. [PubMed: 19972194]
39. Lee H, Xie L, Yu M, Kang H, Feng T, et al. The effect of body posture on brain glymphatic transport. *J Neurosci.* 2015; 35(31):11034–44. [PubMed: 26245965]
40. Iliff JJ, Lee H, Yu M, Feng T, Logan J, et al. Brain-wide pathway for waste clearance captured by contrast-enhanced MRI. *J Clin Invest.* 2013; 123(3):1299–1309. [PubMed: 23434588]
41. Bradbury MWB, Cole DF. The role of the lymphatic system in drainage of cerebrospinal fluid and aqueous humour. *J Physiol.* 1980; 299:353–65. [PubMed: 6155466]
42. Bradbury MW, Westrop RJ. Factors influencing exit of substances from cerebrospinal fluid into deep cervical lymph of the rabbit. *J Physiol.* 1983; 339:519–34. [PubMed: 6411905]
43. Bradbury MW, Cserr HF, Westrop RJ. Drainage of cerebral interstitial fluid into deep cervical lymph of the rabbit. *Am J Physiol Physiol.* 1981; 240:F329–36.

44. Yamada S, DePasquale M, Patlak CS, Cserr HF. Albumin outflow into deep cervical lymph from different regions of rabbit brain. *Am J Physiol Circ Physiol.* 1991; 261:H1197–1204.
45. Mathieu E, Gupta N, Macdonald RL, Ai J, Yucel YH. In vivo imaging of lymphatic drainage of cerebrospinal fluid in mouse. *Fluids Barriers CNS.* 2013; 10:1–5. [PubMed: 23305147]
46. Johnston M, Zakharov A, Papaiconomou C, Salmasi G, Armstrong D. Evidence of connections between cerebrospinal fluid and nasal lymphatic vessels in humans, non-human primates and other mammalian species. *Cerebrospinal Fluid Res.* 2004; 1(2):1–13. [PubMed: 15679934]
47. Louveau A, Smirnov I, Keyes TJ, Eccles JD, Rouhani SJ, et al. Structural and functional features of central nervous system lymphatic vessels. *Nature.* 2015; 523(7560):337–41. [PubMed: 26030524]
48. Aspelund A, Antila S, Proulx ST, Karlsen TV, Karaman S, et al. A dural lymphatic vascular system that drains brain interstitial fluid and macromolecules. *J Exp Med.* 2015; 212(7):991–99. [PubMed: 26077718]
49. Raper D, Louveau A, Kipnis J. How do meningeal lymphatic vessels drain the CNS ? *Trends Neurosci.* 2016; 39(9):581–86. [PubMed: 27460561]
50. Iliff JJ, Wang M, Zeppenfeld DM, Venkataraman A, Plog BA, et al. Cerebral arterial pulsation drives paravascular CSF-interstitial fluid exchange in the murine brain. *J Neurosci.* 2013; 33(46):18190–99. [PubMed: 24227727]
51. Kiviniemi V, Wang X, Korhonen V, Keinänen T, Tuovinen T, et al. Ultra-fast magnetic resonance encephalography of physiological brain activity - Glymphatic pulsation mechanisms? *J Cereb Blood Flow Metab.* 2015:1–13. [PubMed: 25352045]
52. Xie L, Kang H, Xu Q, Chen MJ, Liao Y, et al. Sleep drives metabolite clearance from the adult brain. *Science.* 2013; 342(6156):373–77. [PubMed: 24136970]
53. Lundgaard I, Lu ML, Yang E, Peng W, Mestre H, et al. Glymphatic clearance controls state-dependent changes in brain lactate concentration. *J Cereb Blood Flow Metab.* 2016:1–13. [PubMed: 27233628]
54. Lundgaard I, Li B, Xie L, Kang H, Sanggaard S, et al. Direct neuronal glucose uptake heralds activity-dependent increases in cerebral metabolism. *Nat Commun.* 2015; 6:6807. [PubMed: 25904018]
55. Murlidharan G, Crowther A, Reardon RA, Song J, Asokan A. Glymphatic fluid transport controls paravascular clearance of AAV vectors from the brain. *JCI Insight.* 2016; 1(14):1–11.
56. Thrane VR, Thrane AS, Plog BA, Thiagarajan M, Iliff JJ, et al. Paravascular microcirculation facilitates rapid lipid transport and astrocyte signaling in the brain. *Sci Rep.* 2013; 3:1–5.
57. Maneshi MM, Maki B, Gnanasambandam R, Belin S, Popescu GK, et al. Mechanical stress activates NMDA receptors in the absence of agonists. *Sci Rep.* 2017; 7:1–10. [PubMed: 28127051]
58. Kress BT, Iliff JJ, Xia M, Wang M, Wei H, et al. Impairment of paravascular clearance pathways in the aging brain. *Ann Neurol.* 2014:1–17.
59. Peng W, Achariyar TM, Li B, Liao Y, Mestre H, et al. Suppression of glymphatic fluid transport in a mouse model of Alzheimer's disease. *Neurobiol Dis.* 2016; 93:215–25. [PubMed: 27234656]
60. Gaberel T, Gakuba C, Goulay R, Martinez De Lizarrondo S, Hanouz J-L, et al. Impaired glymphatic perfusion after strokes revealed by contrast-enhanced MRI: A new target for fibrinolysis? *Stroke.* 2014; 45(10):3092–96. [PubMed: 25190438]
61. Wang M, Ding F, Deng S, Guo X, Wang W, et al. Focal solute trapping and global glymphatic pathway impairment in a murine model of multiple microinfarcts. *J Neurosci.* 2017
62. Iliff JJ, Chen MJ, Plog BA, Zeppenfeld DM, Soltero M, et al. Impairment of glymphatic pathway function promotes tau pathology after traumatic brain injury. *J Neurosci.* 2014; 34(49):16180–93. [PubMed: 25471560]
63. Jiang Q, Zhang L, Ding G, Davoodi-bojd E, Li Q, et al. Impairment of the glymphatic system after diabetes. *J Cereb Blood Flow Metab.* 2016:1–12. [PubMed: 27233628]
64. Brightman, M. Ultrastructure of brain endothelium. In: Bradbury, MWB., editor. *Physiology and Pharmacology of the Blood-Brain Barrier.* Berlin Heidelberg: Springer-Verlag; 1992. p. 1-22.

65. Oldendorf W, Cornford M, Brown W. The large apparent work capability of the blood-brain barrier: a study of the mitochondrial content of capillary endothelial cells in brain and other tissues of the rat. *Ann Neurol*. 1977; 1(5):409–17. [PubMed: 617259]
66. Haj-Yasein NN, Vindedal GF, Eilert-Olsen M, Gundersen GA, Skare O, et al. Glial-conditional deletion of aquaporin-4 (Aqp4) reduces blood-brain water uptake and confers barrier function on perivascular astrocyte endfeet. *Proc Natl Acad Sci U S A*. 2011; 108(43):17815–20. [PubMed: 21990350]
67. Cserr HF. Role of secretion and bulk flow of brain interstitial fluid in brain volume regulation. *Ann N Y Acad Sci*. 1988; 529(1):9–20. [PubMed: 3395070]
68. Raichle ME, Hartman BK, Eichling JO, Sharpe LG. Central noradrenergic regulation of cerebral blood flow and vascular permeability. *Proc Natl Acad Sci U S A*. 1975; 72(9):3726–30. [PubMed: 810805]
69. Harik SI. Blood-brain barrier sodium/potassium pump: Modulation by central noradrenergic innervation. *Proc Natl Acad Sci U S A*. 1986; 83(11):4067–70. [PubMed: 3012548]
70. Raichle ME, Grubb RL. Regulation of brain water permeability by centrally-released vasopressin. *Brain Res*. 1978; 143(1):191–94. [PubMed: 415801]
71. Doczi T, Szerdahelyi P, Gulya K, Kiss J. Brain water accumulation after the central administration of vasopressin. *Neurosurgery*. 1982; 11(3):402–7. [PubMed: 7133357]
72. Krieg SM, Sonanini S, Plesnila N, Trabold R. Effect of small molecule vasopressin V1a and V2 receptor antagonists on brain edema formation and secondary brain damage following traumatic brain injury in mice. *J Neurotrauma*. 2014; 31:1–7. [PubMed: 24047225]
73. Zarow C, Lyness Sa, Mortimer Ja, Chui HC. Neuronal loss is greater in the locus coeruleus than nucleus basalis and substantia nigra in Alzheimer and Parkinson diseases. *Arch Neurol*. 2003; 60(3):337–41. [PubMed: 12633144]
74. Raskind MA, Peskind ER, Halter JB, Jimerson DC. Norepinephrine and MHPG levels in CSF and plasma in Alzheimer's disease. *Arch Gen Psychiatry*. 1984; 41(4):343–46. [PubMed: 6703854]
75. Vulchanova L, Schuster DJ, Belur LR, Riedl MS, Podetz-Pedersen KM, et al. Differential adeno-associated virus mediated gene transfer to sensory neurons following intrathecal delivery by direct lumbar puncture. *Mol Pain*. 2010; 6(31):1–9. [PubMed: 20089138]
76. Yang L, Kress BT, Weber HJ, Thiyagarajan M, Wang B, et al. Evaluating glymphatic pathway function utilizing clinically relevant intrathecal infusion of CSF tracer. *J Transl Med*. 2013; 11(107):1–9. [PubMed: 23281771]
77. Nedergaard M. Garbage Truck of the Brain. *Science*. 2013; 340(6140):1529–30. [PubMed: 23812703]
78. Louveau A, Da Mesquita S, Kipnis J. Lymphatics in neurological disorders: A neuro-lympho-vascular component of multiple sclerosis and Alzheimer's disease? *Neuron*. 2016; 91(5):957–73. [PubMed: 27608759]

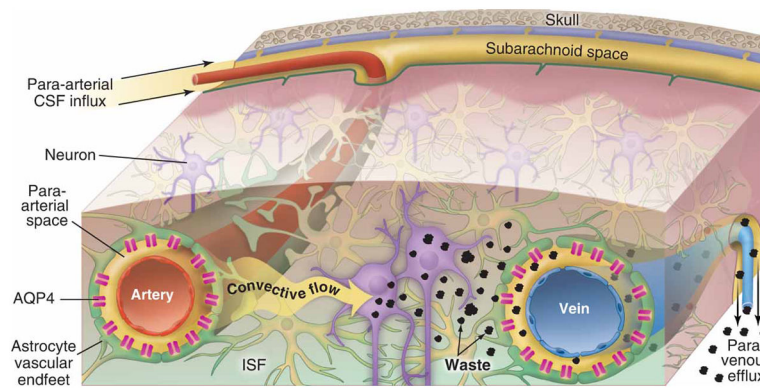


Figure 1. Overview of the circulation of CSF and ISF through the glymphatic pathway
 The bulk flow of CSF into brain specifically within the perivascular spaces of penetrating arteries drives interstitial metabolic waste products toward perivenous spaces, and ultimately from the cranium via several post-glymphatic clearance sites, including arachnoid granulations, meningeal lymphatic vessels, and along cranial and spinal nerve roots. AQP4 water channels densely expressed within astrocyte end-foot processes circumscribing both arteries and veins act to reduce the resistance to CSF movement from periarterial spaces into the interstitium, and from the interstitium into perivenous spaces. Reproduced with permission from (77).

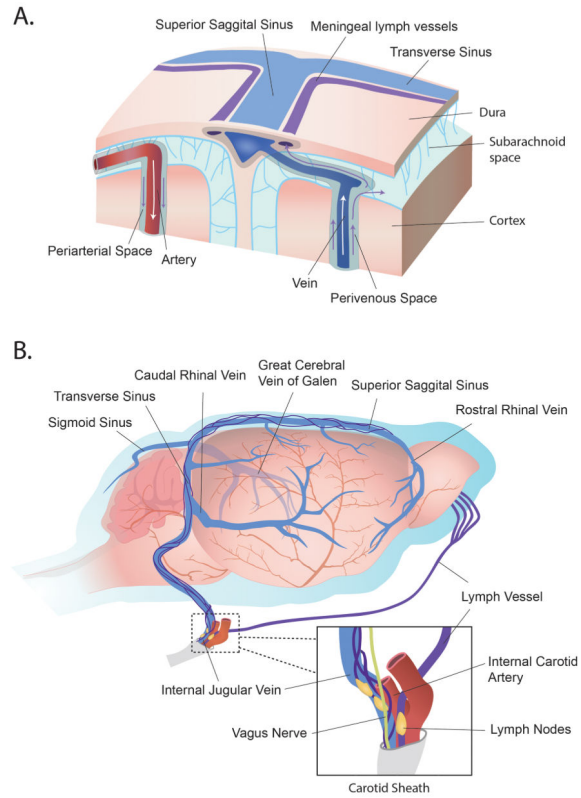


Figure 2. Post-glymphatic clearance pathways
 Glymphatic convective flow is responsible for the drainage of ISF and its constituent solutes, at least in part, to the subarachnoid CSF via perivenous spaces. These solutes can then be cleared to the peripheral venous blood, ultimately to be eliminated in the liver or kidney, by a number of post-glymphatic clearance sites. CSF and waste can pass directly into the venous blood via arachnoid granulations protruding into dural sinuses, such as the superior sagittal sinus (lower left inset). Additionally, macromolecules contained within the CSF can exit the cranium via lymphatic vessels aligning the dural venous sinuses, or alongside olfactory nerves as they traverse the cribriform plate. Both meningeal lymphatics and those positioned within the olfactory mucosa drain to the deep cervical lymph nodes before returning to the venous blood. Reproduced with permission from (78).

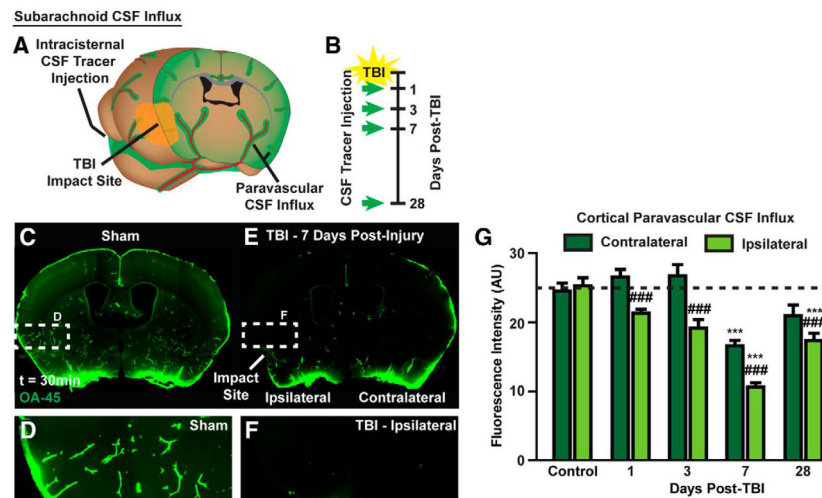


Figure 3. Disruption of glymphatic CSF inflow following traumatic brain injury
 (A and B) At 1, 3, 7 and 28 days following lateral impact murine ‘Hit & Run’ TBI, mice received a cisterna magna injection ($1 \mu\text{L}/\text{min}$, 10 min) of AlexFluor647-conjugated ovalbumin (45 kDa, 0.5% m/v in artificial CSF). After 30 min of tracer circulation, mice were perfusion fixed and cerebral tissues collected to evaluate glymphatic CSF inflow with *ex vivo* conventional fluorescence microscopy. (C–G) Between 1 and 28 days following TBI there was a significant reduction in glymphatic CSF inflow within the hemisphere ipsilateral to the TBI. Interestingly, at 7 days following TBI there was significant global suppression of glymphatic inflow with reduced CSF tracer also seen in the contralateral hemisphere. Reproduced with permission from (62).

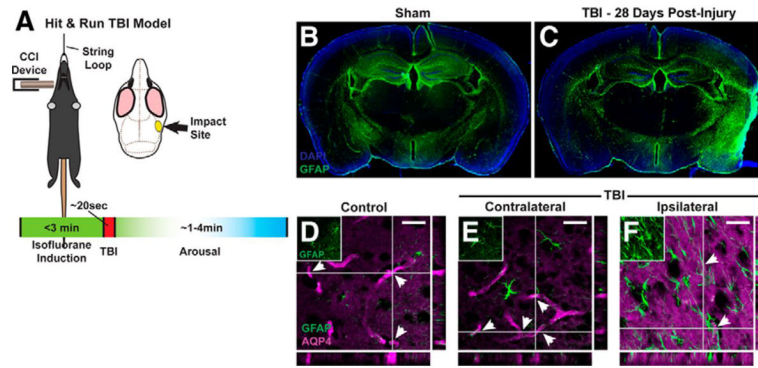


Figure 4. Impaired glymphatic function after traumatic brain injury is associated with astrocytosis and AQP4 mislocalization

(A) Schematic diagram of lateral impact murine ‘Hit & Run’ TBI. (B and C) At 28 days following TBI there was a significant reactive astrocytosis, as measured by increased GFAP expression, surrounding the lesion core and infiltrating the ipsilateral hemisphere to the impact. (D–F) At the same time point, the astrocytic inflammatory state also resulted in mislocalization of AQP4 water channels away from a perivascular distribution, potentially offering a common mechanism between injury, inflammation and glymphatic failure. Reproduced with permission from (62).